Simulation of intercritical annealing in low-alloy TRIP steels

Anthony I. Katsamas, Apostolos N. Vasilakos and Gregory N. Haidemenopoulos

A coupled thermodynamic/kinetic calculation of austenite formation during intercritical annealing of low-alloy TRIP steels is presented. The simulation was performed with the use of Dictra computational kinetics software, which employs a procedure for the numerical solution of the coupled diffusion equations involved, as well as mobility databases for the retrieval of the appropriate kinetic data. Calculated results are compared with available experimental data, in order to evaluate the model. Simulation results, regarding the amount and composition of austenite, the rate of transformation and the effect of annealing temperature and heating conditions, are presented and discussed. It is concluded that the simulation can assist the design of the intercritical annealing in these steels.

Simulation des interkritischen Glühens niedriglegierter TRIP-Stähle. Eine gekoppelte thermodynamische/kinetische Berechnung der Austenitbildung bei einer Glühung niedriglegierter TRIP-Stähle im Zweiphasengebiet wird präsentiert. Die Simulation wurde mit Hilfe der Dictra-Software zur kinetischen Berechnung durchgeführt. Diese Software beinhaltet eine Prozedur für die numerische Lösung der beteiligten gekoppelten Diffusionsgleichung sowie Datenbanken, die Informationen über die Mobilität enthalten, die das Auffinden der passenden kinetischen Daten erleichtern. Berechnete Ergebnisse werden mit vorhandenen gemessenen Daten verglichen, um das Modell zu bewerten. Simulationsergebnisse, die Menge und Zusammensetzung des Austenits sowie die Umwandlungsgeschwindigkeit und die Wirkung von Glühtemperatur und Erwärmungsbedingungen betreffen, werden präsentiert und diskutiert. Es wird der Schluß gezogen, daß die Simulation beim Entwurf der Behandlung im Zweiphasengebiet dieser Stähle behilflich sein kann.

Low-alloy TRIP steels offer excellent combinations of high strength and formability for stretch-forming or deep-drawing applications. The high formability in these steels is attributed to the transformation-induced plasticity of retained austenite. The amount and stability of retained austenite are the key factors, which affect its transformation behaviour during straining. The microstructure of low-alloy TRIP steels typically consists of ferrite, bainite and retained austenite. After cold rolling the steels undergo a two-step heat treatment shown in **figure 1,** consisting of intercritical annealing followed by isothermal annealing at a lower temperature, to stabilize the retained austenite via the bainitic transformation. Much attention has been paid to the second step, i.e. isothermal annealing, since it was realized that bainite transformation temperature and annealing time affect the amount and stability of retained austenite [1...3].

The first step has received much less attention and in most investigations intercritical annealing is performed at a temperature necessary to produce 50% ferrite and 50% austenite. Usually this temperature is established either experimentally or directly read off the Fe-C phase diagram. It is very important, however, to consider phase transformations which occur upon heating, because the microstructural state after intercritical annealing, i.e. volume fraction, chemical composition and homogeneity of austenite, has a great influence on the kinetics of bainite transformation during the isothermal annealing step and, thus, on the stability of retained austenite.

A thorough experimental study of austenite formation during intercritical annealing has been performed in the past by Speich et al. [4] while emphasis was placed on the role of the initial microstructure. In recent years, computational alloy thermodynamics and kinetics have enabled the simulation of the microstructural evolution during heat treatment under either isothermal or continuous heating conditions. Numerical models have been developed [5] for the solution of the diffusion equations, which enable the prediction of austenite formation during heating of hypoeutectoid steels. In the present work, simulation of intercritical annealing is presented. Predictions of the amount of austenite formed, as a function of annealing time and temperature, are compared with available experimental data. The simulations were performed with the Dictra method [6], employing a coupled thermodynamic/kinetic model for the solution of the relevant diffusion equations.

The model

It is well established, e.g. in [4], that austenite formation during heating of ferrite/pearlite mixtures proceeds in two kinetically distinct steps. The first step is very fast and involves the formation of austenite from pearlite. The second step is much slower and involves the formation of austenite from proeutectoid ferrite. In the model presented here, the assumption is therefore that pearlite transforma-

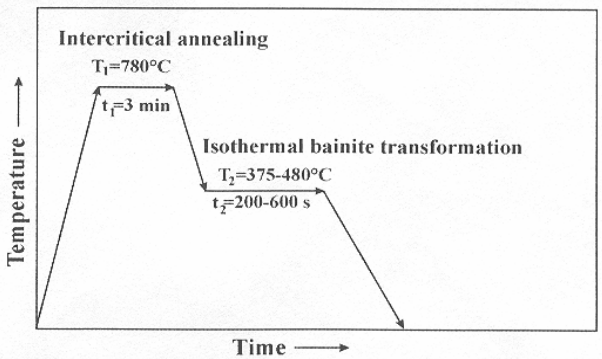

Figure 1. Schematic representation of the two-stage heat treatment typically applied in TRIP steels

Dipl.-Ing. Anthony I. Katsamas; Dipl.-Ing. Apostolos N. Vasilakos, Dr.-Ing. Gregory N. Haidemenopoulos, Associate Professor, Department of Mechanical and Industrial Engineering, University of Thessaly, Volos, Greece.

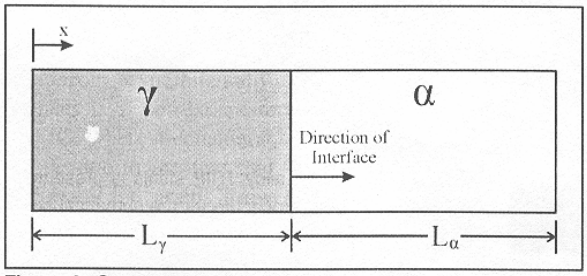

Figure 2. Geometrical model for austenite formation during intercritical annealing

tion to austenite is completed in a negligible amount of time. The conditions at the end of the first step (i.e. volume fractions and compositions) are considered as initial conditions for the second step. Consequently, the system is considered to initially consist of high-carbon γ-austenite (formed from pearlite) and proeutectoid α-ferrite regions, shown in **figure 2.** The model is one-dimensional and a planar geometry is assumed. Thus, the initial widths of the two regions, L_γ and L_α, can be directly related to the volume fractions of the two phases, f_γ and f_α, calculated at a temperature T_s, which corresponds to the temperature where all pearlite has been dissolved and only γ and proeutectoid α remain in the system:

$$\frac{f_\gamma}{f_\alpha} = \frac{L_\gamma}{L_\alpha}. \tag{1}$$

The volume fractions f_γ and f_α are calculated with the aid of computational alloy thermodynamics software Thermo-Calc [7] at T_s, and consequently if L_α is measured by quantitative metallography (proeutectoid ferrite grain-size measurement), then L_γ can be calculated by equation (1). Furthermore, the initial composition of the two phases is also calculated by Thermo-Calc. The initial size and composition of the two phases conform to the nominal composition of the steel via the equation:

$$L_\alpha \cdot c_k^\alpha + L_\gamma \cdot c_k^\gamma = (L_a + L_\gamma) \cdot c_k^o \tag{2}$$

where c_k^α and c_k^γ the concentration of element k in phases α and γ, respectively, and c_k^o the nominal concentration of element k in the steel.

Austenitization is simulated by solving the coupled diffusion equations in the two phases involved. The evolution of concentration profiles of species k, as a function of time in each phase i, $c_k^i(x,t)$, is described by Fick's second law:

$$\frac{\partial c_k^i}{\partial t} = \frac{\partial}{\partial x}\left(D_k^i \frac{\partial c_k^i}{\partial x} \right) \tag{3}$$

where c_k^i is the concentration and D_k^i the diffusion coefficient of species k (C, Mn or Si) in phase i (γ or α). The flux of atoms in a multicomponent system with, say, n components is given by Onsager's extension of Fick's first law [8]:

$$J_k^\gamma = -\sum_{j=1}^{n} D_{jk}^\gamma \frac{\partial c_j^\gamma}{\partial x} \tag{4a}$$

in the austenite-γ region and

$$J_k^\alpha = -\sum_{j=1}^{n} D_{jk}^\alpha \frac{\partial c_j^\alpha}{\partial x} \tag{4b}$$

in the ferrite-α region. Onsager's law accounts for the diffusive flux of a species k, triggered by the existence of a concentration gradient of another species.

Calculation of the γ/α interface velocity, v, is achieved by applying a mass balance to the interface, which is given by the following equation:

$$v \cdot \left({}^{\gamma}c_k^{\gamma/\alpha} - {}^{\alpha}c_k^{\gamma/\alpha} \right) = D_k^\alpha \left(\frac{\partial c_k^\alpha}{\partial x} \right)_{\gamma/\alpha} - D_k^\gamma \left(\frac{\partial c_k^\gamma}{\partial x} \right)_{\gamma/\alpha}. \tag{5}$$

In equation (5), v denotes the velocity of the interface, while D_k^γ and D_k^α are the diffusion coefficients of species k in the two phases. The diffusion coefficients are temperature and concentration dependent and are calculated using the kinetic data available in Dictra. ${}^{\gamma}c_k^{\gamma/\alpha}$ and ${}^{\alpha}c_k^{\gamma/\alpha}$ are the concentrations of k at the γ and α sides of the interface, respectively. These concentrations are calculated by Thermo-Calc, under the assumption that the phases are in local thermodynamic equilibrium at the interface (diffusion controlled transformation). Finally, the index γ/α in the concentration gradients on the right part of equation (5) denotes that gradients are taken on the interface.

The system is considered not to exchange matter with the surroundings, resulting in the following boundary conditions:

$$\left.\frac{\partial c_k}{\partial x}\right|_{x=0} = 0, \tag{6a}$$

$$\left.\frac{\partial c_k}{\partial x}\right|_{x=L_\gamma+L_\alpha} = 0. \tag{6b}$$

Finally, the initial conditions express the concentration of solute atoms in γ and α at the starting temperature T_s, and are given by the following equations:

$$c_k^\gamma(x,0) = c_k^\gamma(T_s), \quad 0 \le x \le L_\gamma, \tag{7a}$$

$$c_k^\alpha(x,0) = c_k^\alpha(T_s), \quad L_\gamma \le x \le L_\gamma + L_\alpha. \tag{7b}$$

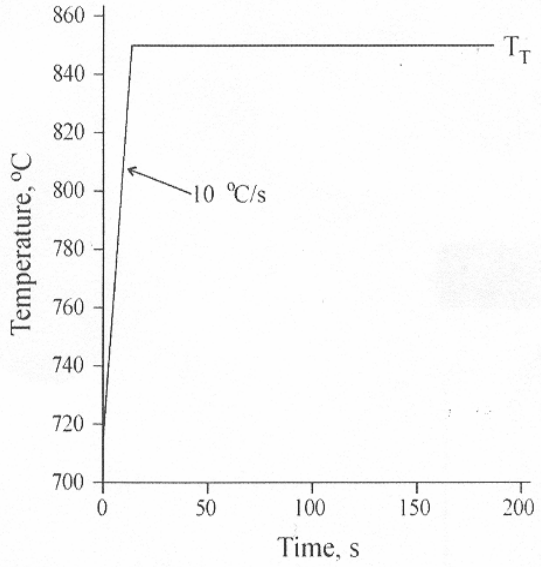

Figure 3. Temperature-time history used in the simulation of intercritical annealing

Table 1. Chemical composition of the TRIP steels used in experiments and calculations (mass contents in %)

	C	Mn	Si
Steel 1	0.142	1.35	1.31
steel 2	0.176	1.41	1.45
steel 3	0.146	1.33	1.28
steel 4	0.174	1.45	1.10

The initial concentrations $c_k^{\gamma}(T_s)$ and $c_k^{\alpha}(T_s)$ are calculated by Thermo-Calc, as mentioned earlier. This 1-D moving boundary problem is solved by using the finite differences method, employing a numerical method for the solution of coupled diffusion equations developed by Ågren [9], which is incorporated in the Dictra computational kinetics software.

Additionally, in order to simulate the intercritical annealing procedure as realistically as possible, the temperature was allowed to increase in a linear manner from the starting temperature T_S, up to the target annealing temperature, T_T, **figure 3:**

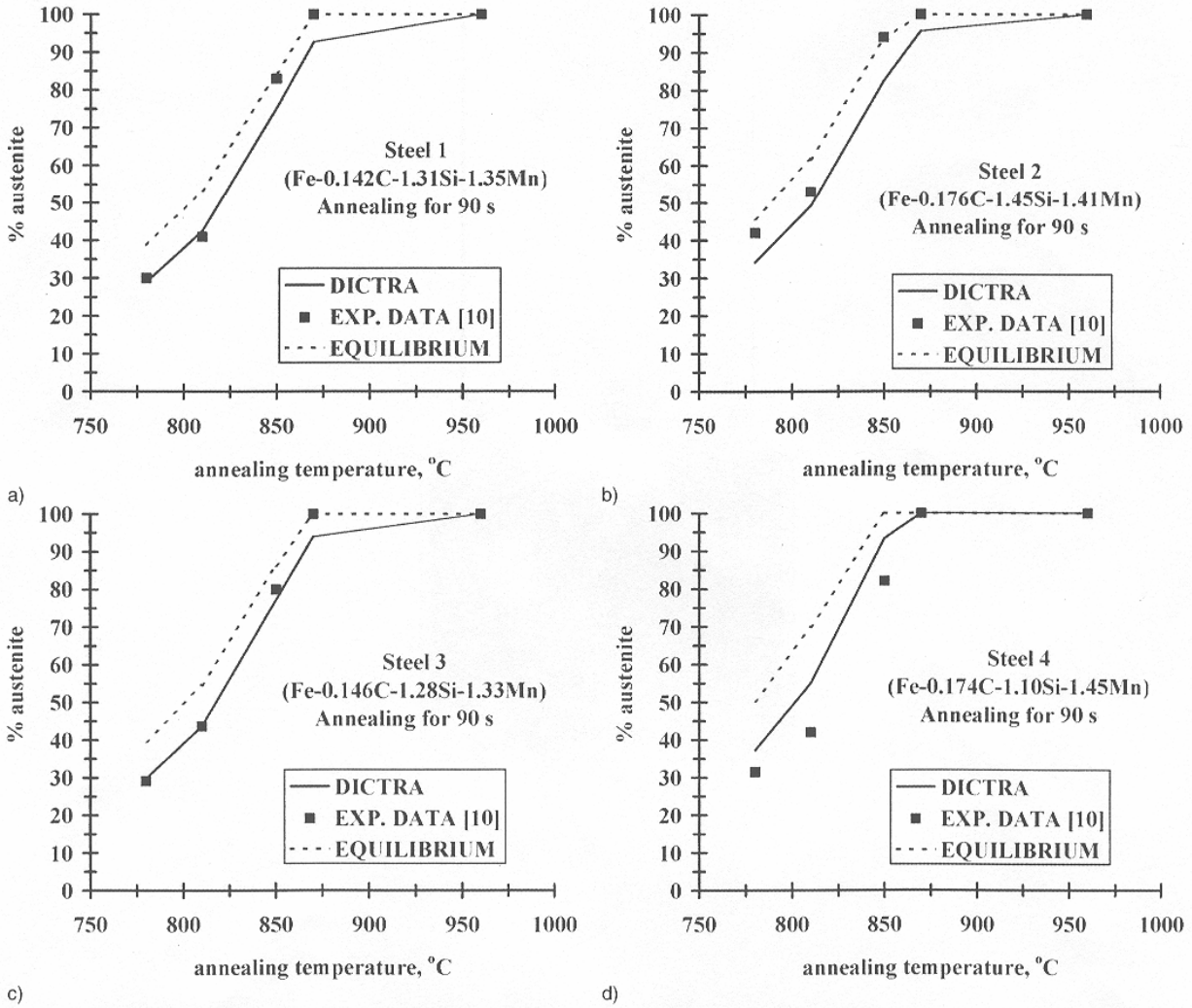

Figure 4. Comparison between the experimentally measured (square symbols) and the calculated (full line) austenite volume fractions in% for steels (a) 1, (b) 2, (c) 3, and (d) 4, after annealing for 90 s at various temperatures. The equilibrium austenite volume fraction in% (dashed line) is also depicted

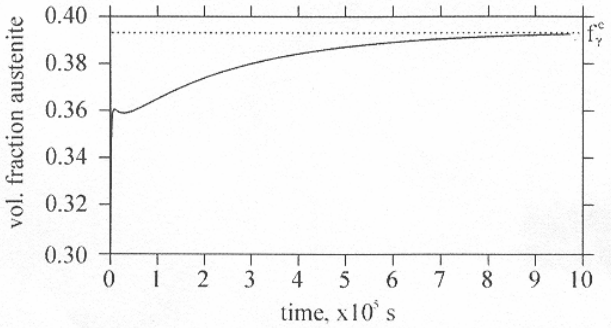

Figure 5. Austenite volume fraction as a function of annealing time for steel 3 at 780 °C

$$T(t) = T_s + 10 \cdot t, \quad 0 \le t \le t_T \tag{8a}$$

$$T(t) = T_T, \; t > t_T \tag{8b}$$

where t_T is the time when the target annealing temperature is reached. A value of 10 °C/s was chosen as a good estimate of the heating rate encountered during such a process.

Results and discussion

Simulation of intercritical annealing was carried out for four different TRIP steels, with chemical composition as shown in **table 1,** for which experimental measurements of the amount of austenite formed were available [10]. The annealing temperatures of the experiments were at 780, 810, 850, 870 and 960 °C. The same target temperatures were also employed in the calculations, in order to allow for a direct comparison of the results. Proeutectoid ferrite grain size was measured by quantitative metallography and found to be approximately 4 μm. Thus, a value of L_α = 2 μm was used in the calculations.

Figure 4a to d depicts the comparison between calculated (full lines) and experimentally measured (square symbols) volume fractions of austenite in % for each steel, as a function of annealing temperature, for a holding time of 90 s. It can be observed that the agreement is fairly good. The diagrams show that at the lower annealing temperatures (780, 810 °C) experimental and calculated values match very well, whereas at higher temperatures the quantity of austenite formed is somewhat higher than the model prediction.

It is also interesting to compare the calculated and measured amounts of austenite with those predicted by equilibrium. The dotted lines in figure 4a to d depict the equilibrium volume fractions of austenite in % for each steel and annealing temperature, as calculated with the aid of Thermo-Calc. As regards the kinetically calculated and equilibrium values, it seems that for all the steels and annealing temperatures considered here, kinetics predict significantly less austenite than thermodynamics. It can be observed that, with only the exception of steel 4, the experimentally measured fraction of austenite lies between the kinetically and the thermodynamically calculated curves. Thus, it seems as if kinetics and thermodynamics set a lower and an upper limit, respectively, within which the experimental results are contained.

Equilibration has proven to be a process requiring substantially greater amounts of time in order to be achieved. **Figure 5** depicts the variation of volume fraction austenite with time for steel 3, annealed at 780 °C. Times up to 10^6 s are required to establish the equilibrium volume fraction, f_γ^e, at the system. This comes in contrast to the usual practice of selecting the annealing temperature for TRIP steels based on thermodynamics, and shows the need to employ kinetics in order to achieve the desired amounts of austenite in the system.

Kinetics simulation also offers a possibility to study the rate of transformation, in an effort to determine the effective stages of the intercritical annealing process. This can be done by examining the velocity of the γ/α interface with respect to time. **Figure 6** presents a typical diagram of v as a function of time, for steel 3 annealed at 810 °C. The

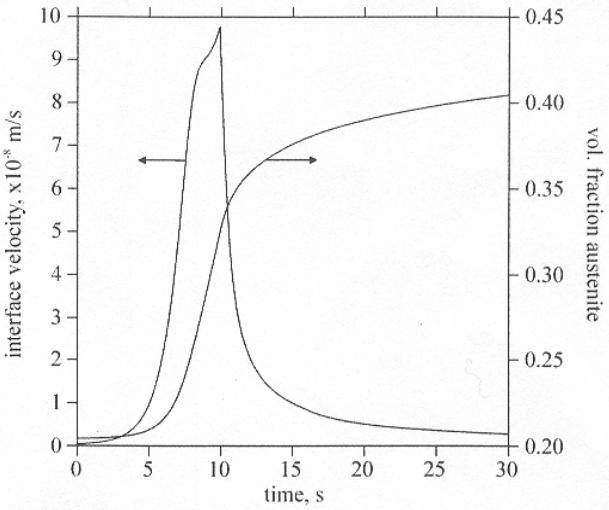

Figure 6. Interface velocity and austenite volume fraction as functions of annealing time for steel 3 at 810 °C

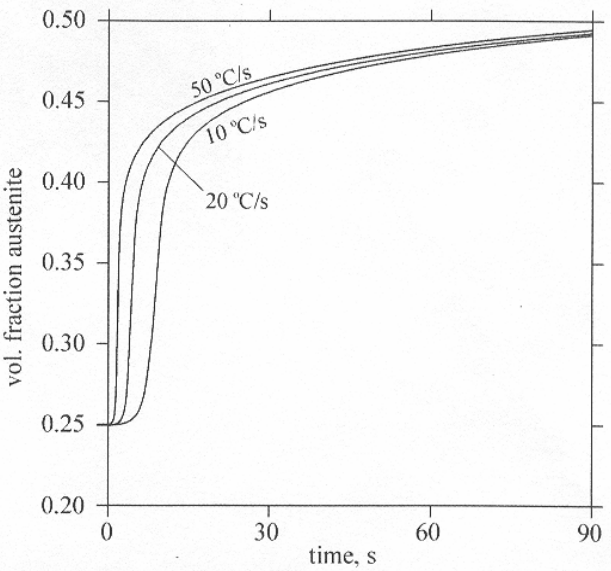

Figure 7. Effect of different heating rates on the volume fraction of austenite for steel 2 annealed at 810 °C

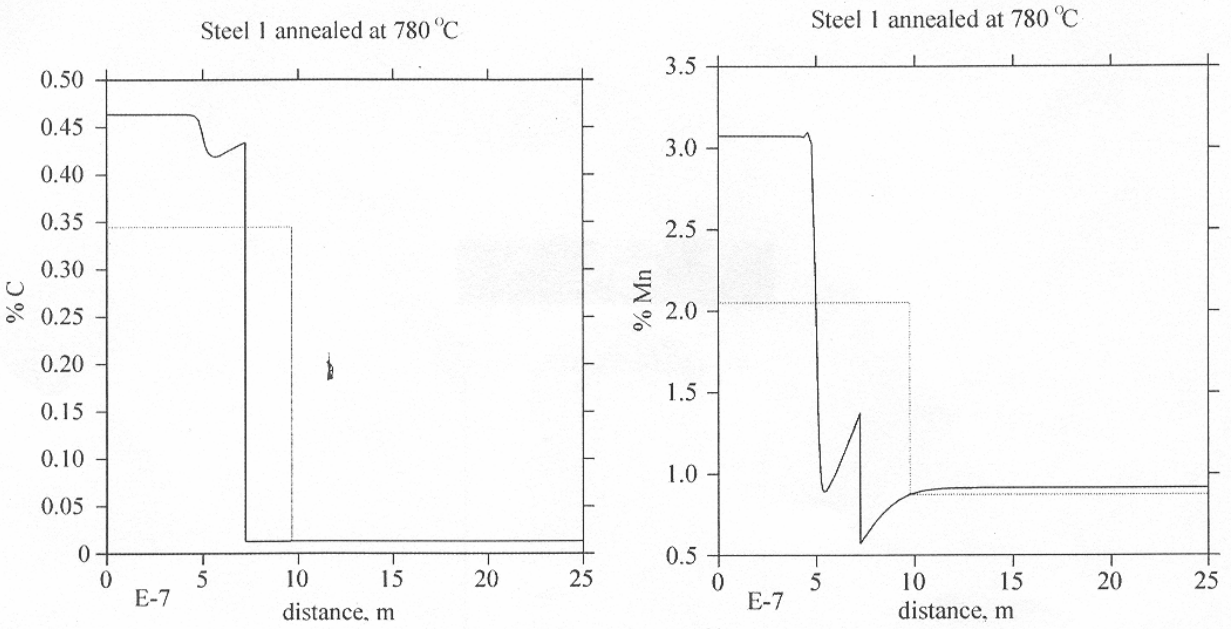

a) b)

Figure 8. Concentration profiles for (a) C and (b) Mn mass contents in % in steel 1, after annealing at 780 °C for 90 s. Dotted line depicts the corresponding equilibrium concentration profiles

corresponding volume fraction austenite is also depicted in the same diagram. It can be seen that interface velocity reaches a maximum value, which occurs at the time when temperature reaches the target annealing temperature. As temperature stabilizes, interface velocity decreases rapidly. The amount of austenite formed during the increase of temperature is not negligible. In the example of figure 6, austenit volume fractions of approximately 10 % form before temperature reaches the target value. Thus, the way by which target temperature is achieved may play some role in the process. For this reason, calculations were performed using different heating rates. **Figure 7** shows the volume fraction of austenite in steel 2 annealed at 810 °C, when heating at a rate of 10, 20 and 50 °C/s, respectively. These calculations show that, in the early stages of the transformation, higher heating rates produce higher amounts of austenite per unit time. However, as time elapses, the effect of heating rate fades and the curves converge.

Another interesting result of the kinetics simulation is the concentration profile diagrams, which show the redistribution of the alloying elements during the transforma-

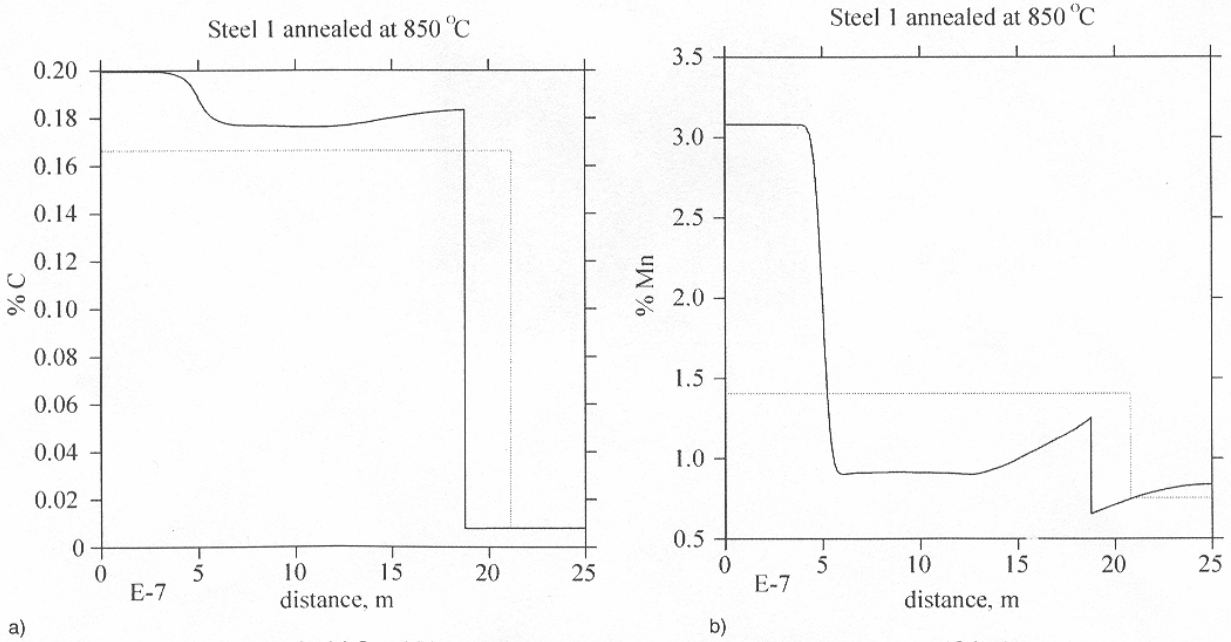

a) b)

Figure 9. Concentration profiles for (a) C and (b) Mn mass contents in % in steel 1, after annealing at 850 °C for 90 s

tion. **Figure 8a** shows the concentration profile diagram for C in steel 1 annealed at 780°C for 90 s, while **figure 8b** shows the corresponding diagram for Mn. The equilibrium concentration profile is also depicted in the diagrams (dotted line). It can be seen that for both C and Mn the concentration profiles are different from that of the equilibrium. Actually, austenite formed during the intercritical annealing transformation is more enriched in carbon and manganese than if equilibration had been achieved. Thus, although the amount of austenite formed is smaller than expected solely by thermodynamic considerations, it is more enriched in carbon and manganese, resulting in enhanced austenite stability. This can lead to more stable retained austenite at the final microstructure, i.e. after the isothermal bainite transformation step.

Figure 9a, b depicts the corresponding concentration profiles for the same steel, but after annealing at 850 °C. It can be seen that austenite is now occupying a higher volume fraction, but is considerably poorer in C than in the case of figure 8a, with an associate reduction in stability. On the other hand, Mn concentration profiles do not differ significantly in figures 8b and 9b, despite the large difference of the annealing temperatures. This is clearly a result of the sluggish way in which Mn diffuses during the transformation. The high Mn content of austenite is inherited from formerly pearlitic regions, which transform to austenite in the first stage of austenitization. It seems, therefore, that C plays the most important role in austenite stabilization, since Mn needs significantly longer times than the ones usually employed in the intercritical annealing of TRIP steels, in order to redistribute in austenite.

Conclusions

Computational kinetics modelling of austenite formation, during the intercritical annealing of TRIP steels, leads to the following concluding remarks:

- the experimentally measured and the calculated volume fractions of austenite, formed during intercritical annealing, are in good agreement. In most of the cases studied in this work, experimental results are placed between a lower limit set by kinetic calculations, and an upper limit set by equilibrium (thermodynamic) calculations;
- the equilibrium amount of austenite is obtained at times significantly longer than the ones usually employed during the intercritical annealing of TRIP steels. Thus, selection of the appropriate annealing temperature solely by the Fe-C phase diagram may actually lead to less austenite than desired;
- a significant portion of austenite is formed, as the steel is heated towards the target annealing temperature. Higher heating rates seem to increase the amount of austenite formed at the early stages of the transformation, whereas at later stages the effect of heating rate fades away, as austenite tends to reach its equilibrium value;
- examination of the calculated concentration profiles reveals that austenite is enriched in C and Mn, especially at low annealing temperatures. This enhances the stability of austenite, which is crucial for the TRIP behaviour of the steel. At higher annealing temperatures, the enrichment of austenite in C is reduced. On the contrary, Mn enrichment is retained due to its substantially lower mobility;
- computational kinetics modelling of austenite formation can be used as a powerful tool, for a more accurate design of the intercritical annealing treatment, during the processing of TRIP steels.

(A 01 593; received: 12. May 2000)

References

[1] *Matsumura, O.; Sakuma, Y.; Takechi, H.:* Trans. ISIJ 27 (1987), p. 570/79.

[2] *Haidemenopoulos, G.; Papadimitriou, K.:* steel res. 66 (1995) No. 10, p. 433/38.

[3] *Vasilakos, A.N.; Papamantellos, K.; Haidemenopoulos, G.N.; W. Bleck, W.:* steel res. 70 (1999) No. 11, p. 466/71.

[4] *Speich, G.R.; Demarest, V.A.;. Miller, R.L.:* Metall. Trans. 12A (1981), p. 1419/28.

[5] *Jacot, A.; Rappaz, M.:* Acta Mater. 45 (1997) No. 2, p. 575/85.

[6] *Ågren, J.:* ISIJ Inter. 32 (1992) No. 3, p. 291/96.

[7] *Sundman, B.; Jansson, B.; Andersson, J.-O.:* CALPHAD 9 (1985), p. 153.

[8] Dictra – Course Material, Div. of Physical Metallurgy, Royal Institute of Technology, Stockholm.

[9] *Ågren, J.:* A new numerical method to solve coupled diffusion equations, intern. rep. ser. D, No. 84, Institutionen för Metallografi, KTH, Stockholm, 1987.

[10] *Papamantellos, K.:* Umwandlungsverhalten und mechanisch-technologische Eigenschaften von niedriglegierten TRIP-Stählen, Aachen, 1998 (Ph.D. thesis).